

## List of Corrections

# Determination of Shear Modulus using Seismic Cone Penetration Test in Northern Denmark

Jeremy Geron      Alexandra-Ioana Iliescu

08.06.2012

## Abstract

The initial application of CPTu and SCPTu results is to evaluate soil type soil and stratigraphy. Several charts such as, Robertson et al. (1986) and Robertson (1990) where generated to obtain in an easy way accurate results. Several theoretical methods where use to interpretate the obtained data. The most common CPTu methods to estimate soil type are the ones suggested by Robertson based on cone resistance,  $q_c$ , friction ratio,  $R_f$  and normalized parameters. In this article it has been decide to compare the Shear Modulus  $G_{max}$  obtained from the Seismic Cone Penetration Test to the Shear Modulus  $G_0$  obtained from the ordinary Cone Penetration Test.

*Keywords:* shear modulus, seismic, cone penetration test, shear velocity

## 1 Introduction

The geotechnical investigation has been increasing, for a few decades now, mainly because of the many engineering problems in which the dynamic behaviour of soil is significant. The interested has pushed the people to develop new analytical and dynamic testing methods. On sites CPTu and SCPTu have become standard techniques for dynamic testing to determine the in situ shear wave velocity. After a in situ test, that consist on a geophone integrated in a cone that will measure the waves generated by a shock between a hammer and a steel plate. A polirezed shear wave is generated and the time is measured for the shear wave to travel a know distance to the geophone in the borehole. Elastic theory relates the shear Modulus,  $G_{max}$ , soil density  $\rho$ , and the shear wave velocity,  $V_s$

$$G_{max} = \rho V_s^2 \quad (1)$$

From this formula the shear modulus can be determined using SCPTu.

## 2 Different types of waves

### 2.1 Introduction

Characterization of the soils by seismic techniques is to observe a wave field, measuring propagation properties, and via a process of interpretation, a distribution of subsurface properties that influence propagation. This can be realized using different techniques and acquisition geometries. Seismic geophysical methods most used are based on the propagation of body

waves. In this context, surface waves generate noises that have to be attenuated. The surface waves can be interpreted and even be acquired specifically to characterize the subsurface was shallow.

### 2.2 Different type of waves.

There are several types of waves. They are grouped into two categories used in the field of geology. The former are the plane waves or body waves. The theory shows that the elastic homogeneous solids under the effect of stress (Shaking), the homogeneous and isotropic elastic solid undergoing deformation are then two main types of waves (O. and Y.) They move, either longitudinally (it is the compression waves or P waves) or transverse (shear waves or S waves). Figure 1 shows the propagation associated with these waves.

$$V_p = \sqrt{\frac{\lambda + 2\mu}{\rho}} \quad (2)$$

and,

$$V_s = \sqrt{\frac{\mu}{\rho}} \quad (3)$$

where,

- $\lambda$ : Lamé coefficients [MPa]
- $\mu$ : Lamé coefficients [MPa]
- Shear modulus,  $G$
- $\rho$ : density [kg/m<sup>3</sup>]

The longitudinal and transversal ratio can be then written :

$$\frac{V_p}{V_s} = \sqrt{\frac{\lambda + 2\mu}{\mu}} \quad (4)$$

where,  $\lambda$  and  $\mu$  being positive, the ratio is at least equal to  $\sqrt{2}$ .

The second category of waves corresponds to the surface waves. It is the Rayleigh waves, their displacement is in the vertical plane of propagation and possessing both a longitudinal and a transverse component (similar to the waves). But also the Love waves are part of the surface waves. Finally, to be noted that they are slower than body waves, but their amplitude is higher. The displacement associated with surface waves is shown in Figure 1.

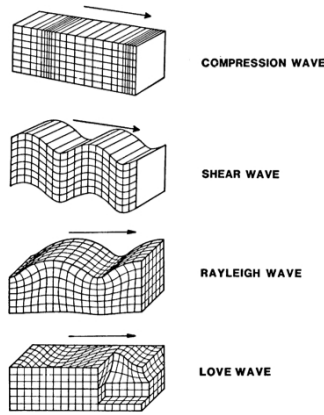


Figure 1: Different types waves. (Rice, 1984)

If an approximation of the intensity of these waves it has been proved that 67% of the total energy propagates in the Rayleigh waves, which means that only 26% are propagated as Shear waves (S) and 7% as Compression (P) waves as stated in (D.). The fact that two thirds of the energy is Rayleigh but also the shear and the compression waves amplitude decreases faster than the Rayleigh. These two different waves are the most specific waves for this test.

### 2.3 S-waves and P-waves.

The Shear wave are measurements that are taken at the surface of the earth. The direction of the Shear wave for a particle vibration can be conveniently divided into two components one component parallel to the surface (SH) and a the second one in the vertical direction (SV). Seismic sources for shear wave generation in engineering investigations are often designed to generate either dominantly P and SV or dominantly SH waves. The reason lies in the fundamentally different behavior of SV and SH waves at a boundary. If an SH wave strikes a horizontal geologic discontinuity, part of the energy is transmitted

through and part is reflected back, but both of the outgoing waves are of the SH type. In contrast, an SV wave striking a horizontal geologic discontinuity will produce four outgoing waves; SV and P; reflected and transmitted.

Similarly a P wave striking a discontinuity will also produce four outgoing waves. Most seismic sources designed to produce SV waves will also produce substantial P waves and most SV detectors will also detect P waves. Thus the observed seismic wave form may include a complicated sequence of arrivals consisting of direct and converted P and SV waves. In contrast, careful design of an SH type seismic source should minimize the interference of other wave arrivals.

Shear waves display a unique characteristic which allows for their accurate identification from other wave types, particularly compressional waves. By reversing the direction of the energy impulse at a bidirectional signal source, oppositely polarized shear waves can be obtained. Also, S-waves are slower than the P-waves, where the P-wave is the one that appear first

P wave is also a measurement taken at the surface of the earth, but this one is faster than the shear wave so it is the first one to arrive to the observation point. This is the reason it is also called the primary wave. The mode of propagation of a P wave is always longitudinal; thus, the particles in the solid have vibrations along or parallel to the travel direction of the wave energy.

## 3 Shear modulus

The shear modulus is one of several parameters for measuring the stiffness of materials. All of them arise in the generalized Hooke's law: Young's modulus describes the material's response to linear strain (like pulling on the ends of a wire), the bulk modulus describes the material's response to uniform pressure, and the shear modulus describes the material's response to shearing strains.

### 3.1 Shear modulus Obtained from SCPT

The dynamic shear modulus,  $G_{max}$ , is generally found using the Geotechnical method of Seismic Cone penetration test. The Shear wave velocity is obtained from this SCPT and after laboratory test the relevant density is found and the shear modulus can then be found as seen in Equation(3).

The shear modulus is largest at low strains and decreases with increasing shear strain (Seed

and Idris). The shear strain amplitude in Seismic test is usually low. Which allow to find the very low strain level of dynamic shear modulus,  $G_{max}$ .

To obtain the dynamic shear modulus a seismometer is placed in the horizontal direction and orientated transverse to the signal source to detect the different components of the shear wave (horizontal and transversal). The ideal seismic signal source should generate a large amplitude shear wave with little or no compressional wave component. The signal can be generated by a hammer hitting a plate.

To obtain the measurements a rugged velocity seismometer has been incorporated into the cone penetrometer. It is placed in the horizontal direction and oriented transverse to the signal source to detect the horizontal component of the shear wave arrivals. The most suitable seismic signal source should be generated a large amplitude  $S$  wave with a small compressional wave.

### 3.2 Shear Modulus obtained from CPT

The shear modulus,  $G_0$  in a coarse soil layer is determined using the Equation 5 from (R. G. Campanella).

$$\frac{G_0}{q_c} = 1634 \left( \frac{q_c}{\sqrt{\sigma'_{v0}}} \right)^{-0.75} \quad (5)$$

where,

$$\begin{aligned} q_c: & \text{Cone resistance} & [MPa] \\ \sigma'_{v0}: & \text{Effective overburden stresses} & [MPa] \end{aligned}$$

For this paper, the shear modulus,  $G_0$ , in a fine soil layer is determined can be determined by Equation 6 from (R. G. Campanella).

$$G_0 = 99.5(p_a)^{0.305} \frac{(q_t)^{0.695}}{(e_0)^{1.130}} \quad (6)$$

$$\begin{aligned} p_a: & \text{Atmospheric reference stress} & [MPa] \\ e_0 & \text{in situ void ratio} & [-] \end{aligned}$$

## 4 Interpretation of results

### 4.1 Correction of Measured Data for the CPT

Due to the fact that the cone penetration test is done in in situ it generates errors (stones or soil irregularities, breaks while penetration of the cone, cables unplugged, ect.). These measurements have then to be corrected. The cone resistance and the sleeve friction needs to be corrected in order to account for the specific

cone design, which influences how the pore water pressure alters the measurements. This is in particular important in the soft normally consolidated or low consolidated soil where the pore pressure behind the cone may be large. The cone resistance is corrected using Equation 7, and the sleeve friction is corrected using Equation 8:

$$q_t = q_c + u_2 * (1 - a) \quad (7)$$

$$f_t = f_s - \frac{(u_2 * A_{sb} - u_3 * A_{st})}{A_s} \quad (8)$$

where,

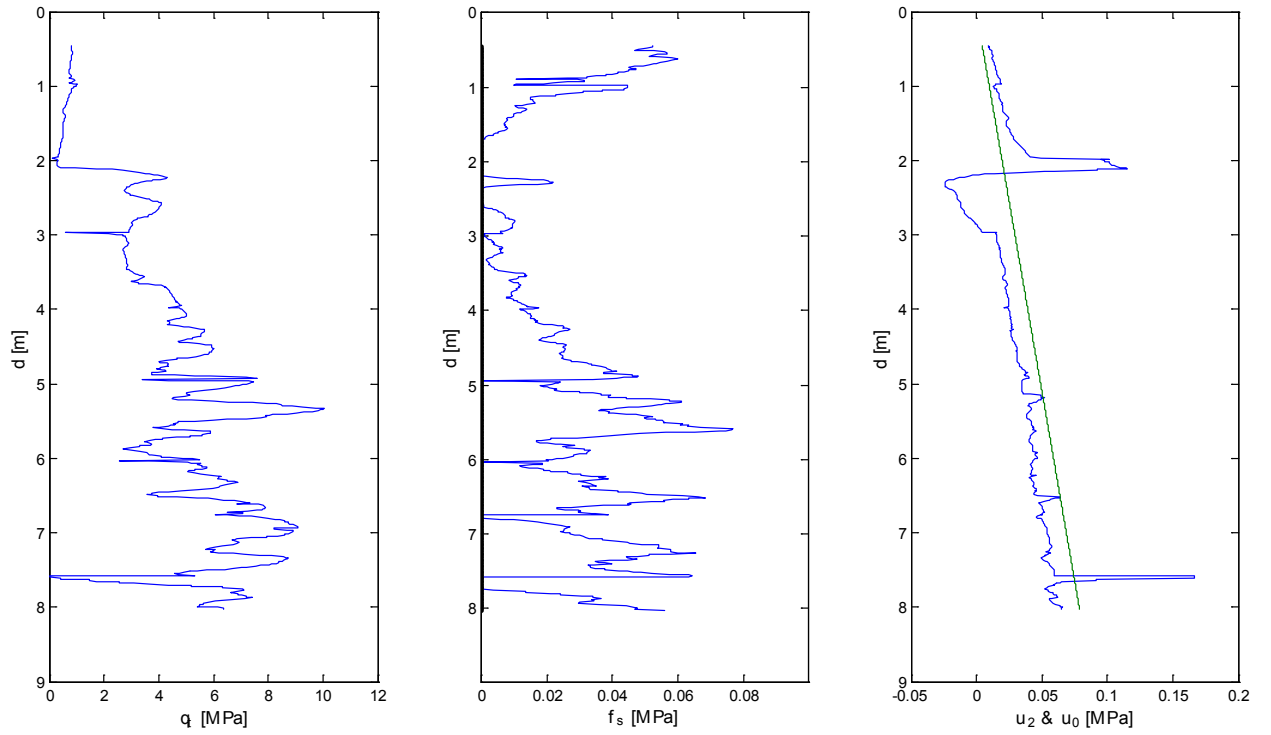
$$\begin{aligned} q_t: & \text{Corrected cone resistance} & [MPa] \\ a: & \text{Cone area ratio} & [a = \frac{A_n}{A_c}] \\ A_n: & \text{Cross section area of the shaft} & [mm^2] \\ A_c: & \text{Cross section area of the cone} & [mm^2] \\ u_2: & \text{Pore pressure behind the cone} & [MPa] \\ f_t: & \text{Corrected sleeve friction} & [MPa] \\ f_s: & \text{Measured sleeve friction} & [MPa] \\ A_{sb}: & \text{Cross section area of sleeve bottom} & [mm^2] \\ A_{st}: & \text{Cross section area of sleeve top} & [mm^2] \\ A_{sb}: & \text{Friction sleeve surface area} & [mm^2] \end{aligned}$$

However it is not always possible to obtain the corrected sleeve friction.

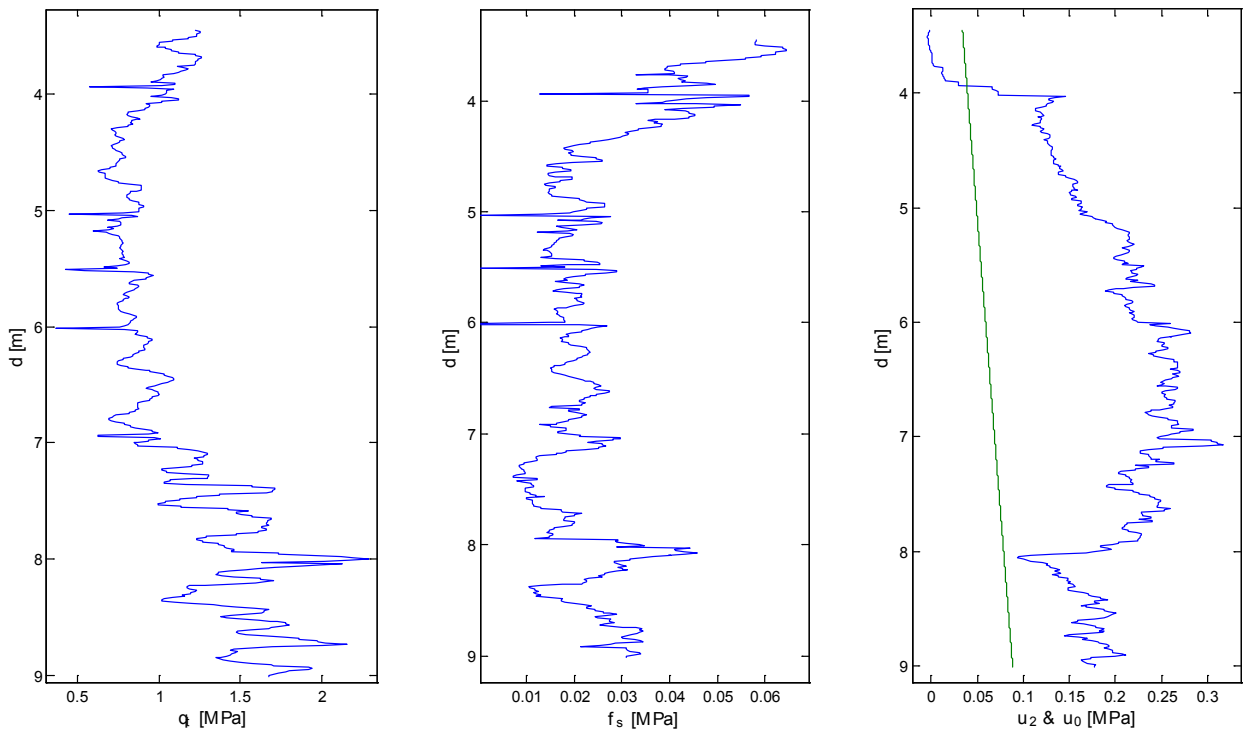
### 4.2 Identification of stratigraphy

First step is to identify the stratigraphy based on the direct measurements. Sand is characterized by a high cone resistance and a low sleeve friction and furthermore, as for the hydrostatic water pressure and pore pressure behind the cone, they are the same. By comparison, clay is characterized by a low cone resistance, high sleeve friction and the hydrostatic water pressure,  $u_0$ , and the pore pressure behind the cone,  $u_2$ , differ. Silt is characterized a like clay due to the behavior in a CPT.

Figure 2 shows the data obtained from the CPTu for sand and clay, (Iliescu and Geron), where  $q_t$ , sleeve friction,  $f_s$ , pore water pressure,  $u_2$  in blue and in green the in situ pore water pressure,  $u_0$ . On the basis of this, the soil is divided in layers. The classification is verified by using Robertson  $R_f - q_t$  and  $B_q - q_t$  diagrams. In order to classify the soil an estimate of the unit soil weight is needed. This is done by an iterative process using two different Robertson interpretation.  $B_q - q_t$  diagram, where the pore pressure ratio,  $B_q$ , is defined by the Equation 9.



(a) Fill, (0-1m), Gytta, (0-3m) and Sand (3-8m) Layer



(b) Clay (3-9m) Layer

Figure 2: CPT results obtained according to (Iliescu and Geron)

$$B_q = \frac{u_2 - u_0}{q_t - \sigma_{v0}} \quad (9)$$

where,

$$\begin{aligned} q_0: & \text{ Hydrostatic water pressure} \quad [MPa] \\ \sigma_{v0}: & \text{ In situ vertical stress} \quad [MPa] \end{aligned}$$

However, since  $B_q$  depends on the in situ vertical stress,  $\sigma_{v0}$ , and hence the unit weight of the soil, a two different estimations of the unit weight are done using the Robertson  $R_f - q_t$  and  $f_r - q_t$  diagrams. The two different interpretation Robertson made are in 1986 and 1990. The chart of 1986 uses the basic CPTu measurements of  $q_c$  and  $f_s$  and has 12 soil types, where as the chart of 1990 uses normalized parameters and has 9 soil types. The different soil type in each chart have sometimes created some confusion when comparing results. The advantage of the early Robertson et al (1986) chart was that it could be used in real-time to evaluate soil type during and immediately after the CPTU, since it only requires the basic CPT measurements. Although the normalized charts of Robertson (1990) are considered more reliable because they use CPT parameters normalized in terms of effective stress, they can only be applied after the CPT during post-processing, since they require information on soil unit weight and groundwater conditions that are not available during the CPTu, (P.K.Robertson).

#### 4.2.1 Robertson 1986

The first classification chart Robertson proposed is based on a simple equation where the relative sleeve friction,  $R_f$  is defined as seen in Equation below 13.

$$R_f = \frac{f_s}{q_c} \quad (10)$$

where,

$$\begin{aligned} R_f: & \text{ Relative sleeve friction} \quad [\%] \\ q_c: & \text{ Cone resistance} \quad [MPa] \end{aligned}$$

According to T. Lunne (1997), generally more reliable soil classification can be made using the corrected total cone resistance,  $q_t$ , sleeve friction,  $f_s$  and the pore pressure,  $u$ . A first attempt was proposed by Roberston et al. (1986), once the relative sleeve friction for every data is known, these can be plotted in a  $R_f - q_t$  diagram in order to estimate the approximate soil unit weight and soil type of each data point, as shown in Figure 3:

The color scale in Figure 3 represent the zones of the soil behaviour type as seen in Table 1. It can be observed that for sand there are several

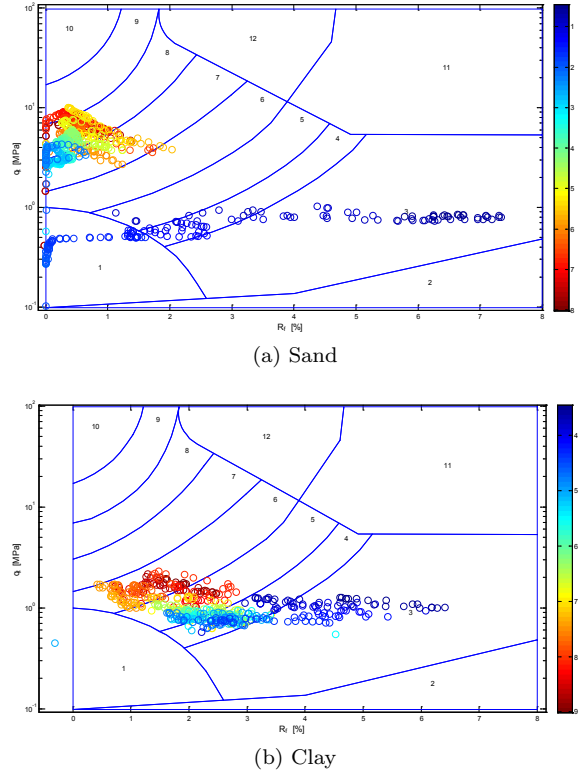


Figure 3: Soil behaviour type classification from CPTu data, according to (T. Lunne, 1997)

types of soil ranging mainly in zone 1,2,4 and 7,8,9, respectively the first 3 meters filled with sensitive fine grained, organic material and clay, and silty sands. For clay the ranges are between zones 3,4,5 and 6, meaning from clay to clayey silts. From the soil classification tests performed in (Iliescu and Geron) it can be stated that the theoretical results are matching the experimental ones, which allows to continue the processing of the data and a accurate choose of formulas. That is why before starting to take a closer look to the data obtained from the CPTu it is important to classify the soil data.

Table 1: Soil type behaviour using Robertson 1986, (T. Lunne, 1997)

Zone	Soil behavior type
1	Sensitive fine grained
2	Organic material
3	Clay
4	Silty clay to clay
5	Clayey silt to silty clay
6	Sandy silt to clayey silt
7	Silty sand to sandy silt
8	Sand to silty sand
9	Sand
10	Gravelly sand to sand
11	Very stiff fine grained
12	Sand to clayey sand

Once an estimate of the soil unit weight has been made, it is possible to calculate the in situ vertical stresses,  $\sigma_{v0}$ , down through the profile and further compute the pore pressure ratio given by Equation 9.

According to (T. Lunne, 1997),  $B_q$  data is often more reliable than the data obtained from the sleeve friction, and each data set can fall into different soil types for a  $R_f - q_t$  and  $B_q - q_t$  diagram and hence change the unit weights,  $\sigma_{v0}$  and finally  $B_q$ . Because of this, each data point is plotted in a Robertson  $R_f - q_t$  diagram, to get a new estimate of the soil unit weight, and this a new pore pressure ratio. This iterative procedure is continued, until no data points experience a change in  $B_q$ .

sure ratio,  $B_q$  are defined as seen in the Equation 13.

$$Q_t = \frac{q_t - \sigma_{v0}}{\sigma'_{v0}} \quad (11)$$

$$f_r = \frac{f_s}{q_c - \sigma_{v0}} * 100\% \quad (12)$$

$$B_q = \frac{u_2 - u_0}{q_t - \sigma_{v0}} \quad (13)$$

where  $\sigma_{v0}$  is

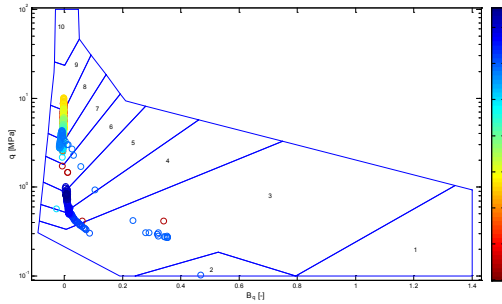
$$\sigma_{v0} = \frac{d * g * \rho_w}{10^6} + \frac{\gamma * d}{10^3} \quad (14)$$

$q_c$ : Cone resistance [MPa]  
 $\sigma_{v0}$  in situ vertical stresses [MPa]

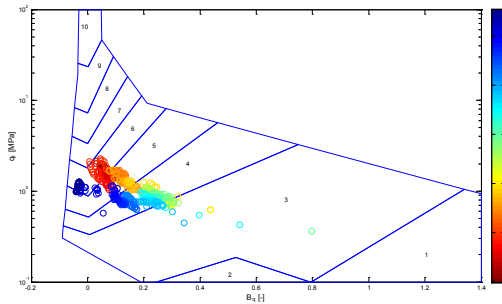
Based on the normalized parameters, Robertson changed the soil behaviour type classification charts in 1990 and gathered them as in Table 2: Once the normalized friction ratio

Table 2: Soil behaviour type classification based on normalized CPTu data after Robertson 1990, (T. Lunne, 1997)

Zone	Soil behavior type
1	Sensitive, fine grained
2	Organic soils-peats
3	Clays-clay to silty clay
4	Silt mixtures clayey silt to silty clay
5	Sand mixtures; silty sand to sand silty
6	Sands; clean sands to silty sands
7	Gravelly sand to sand
8	Very stiff sand to clayey sand
9	Very stiff fine grained



(a) Sand



(b) Clay

Figure 4: Soil behaviour type classification from CPTu data, according to (T. Lunne, 1997)

From the pore pressure parameter,  $B_q$  classification it can be observed that for sand the ranges are more restrained and exact concerning zone classification, the data passing mainly on zone 3,4 and 7,8, silty clay and sandy silt. Concerning clay the data is found in mainly in zone 4,5 and 6 determining from silty clay to clayey silt.

#### 4.2.2 Robertson 1990

The classification charts that Robertson proposed are based on normalized values so, cone resistance,  $Q_t$ , friction ratio,  $f_r$  and pore pres-

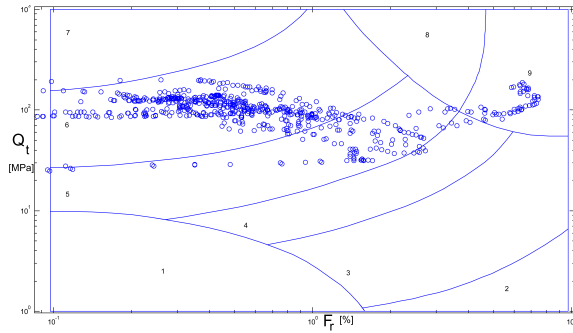
sure ratio, these can be plotted in a Robertson  $Q_t - F_r$  diagram that will allow an other estimation of the approximate soil unit weight and soil type of each data point, as shown in Figure 5:

For sand the data are found mainly in zone 5,6 and 9 which define silty and fine sands. As for clay, the range is between zone 3,4 and 5, respectively, clay, silty clay and silty sand. Negative data for both tests were ignored.

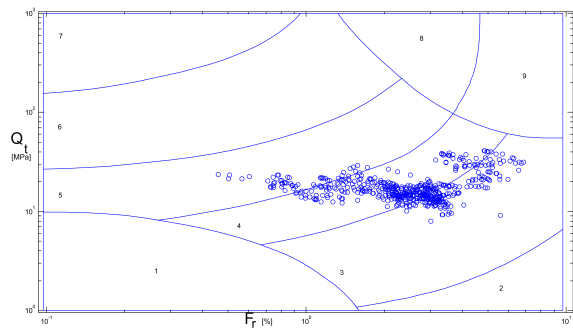
A second chart suggested by Robertson was the  $Q_t - B_q$  one using the same soil type classification zones seen in Table 2 and it can be seen in Figure 6.

It can be observed that for sand the results are found mainly in zone 5 and 6, respectively sand and silty sand, whereas for clay samples, the results are found in zone 3,4 and 5 which define clays, silty clays and silty sand.

In general, the normalized chart (Robertson, 1990) provides more reliable identification of soil

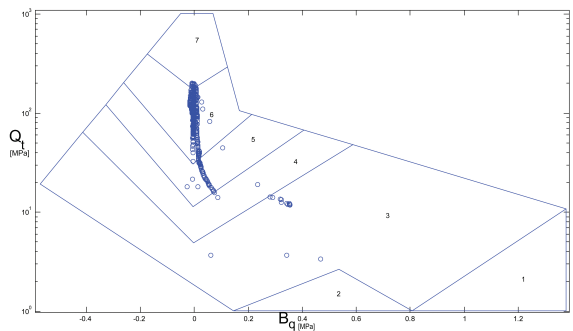


(a) Sand

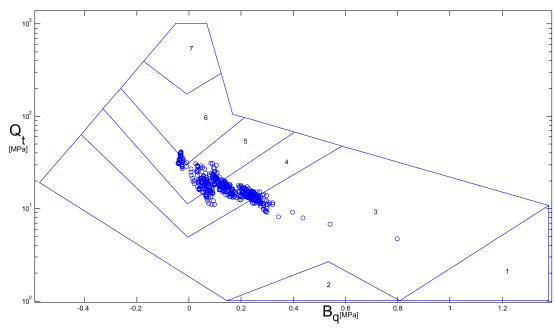


(b) Clay

Figure 5: Soil behaviour type classification from CPTu data, according to (T. Lunne, 1997)



(a) Sand



(b) Clay

Figure 6: Soil behaviour type classification from CPTu data, according to (T. Lunne, 1997)

behaviour type than the non-normalized charts (Roberston, 1986), (T. Lunne, 1997).

### 4.3 Shear Modulus obtained from SCPT

#### 4.3.1 Introduction

To obtain the shear modulus,  $G_{max}$  equation 1 previously mentioned is used. Two different interpretation methods were used to determine the shear velocity  $V_s$ , the methods used are Reverse Polarity and Cross correlation.

#### 4.3.2 Dispersion

Surface waves of varying wavelengths penetrate to different depths and travel at the velocity of the mediums they are traveling through as in Figure 7. This one was generated by plotting the amplitude of surface waves against depth. This was done for two different waves, Left shear wave and Right shear wave and an interpolation is applied.

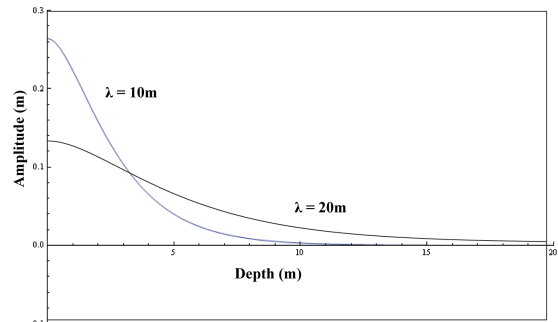


Figure 7: Surface wave penetration (Dobrin, 1951)

When attempting surface wave inversion, phase velocities are used more often than group velocities because it is easier to create a dispersion curve of phase velocities. A dispersion curve is a plot of velocity versus frequency or wavelength.

#### 4.3.3 Data gathering

Two main data gathering techniques are employed in gathering surface wave information. The two methods are spectral analysis of surface waves and multi-channel analysis of surface waves. These techniques use either passive or active sources. Passive sources are simply ambient noise, while active sources include traditional seismic sources such as an explosive device or a steel plate being hit with a hammer. Overall, passive energy sources usually require more time when data gathering than active energy. Ambient noise is also more useful when it



### 4.3.6 Cross-Correlation

The Cross-correlation calculates the time interval by aligning the signal trains in the time axis, and it utilizes considerably more information in the collected shear waves than the first arrival and first cross-over methods. It refers to the correlation of two independent series, and can be used to measure the degree at which the two series are related. where the time shift  $s$  is defined in Equation 16.

$$z(s) = \int_{-\infty}^{\infty} x(t)y(t+s)dt \quad (16)$$

$x(t)$ : continuous signals  
 $y(t)$ : with respect of time  
 $s$ : time shift

For two signals of the same shape, the cross-correlation function may be used to calculate their difference in their arrival times, which is equal to the time shift that results in the peak of the cross-correlation function. Originally, the cross-correlation was done in the frequency domain, since it required relatively little computation time compared with that done directly in time domain. However, with the computer speed having doubled, computation time in the time domain has become insignificant. It is sometimes more advantageous to do cross-correlation in a statistical way in the time domain, since its physical meaning is clear and it can provide some regression parameters to evaluate the quality of the process. In the Equation 17 the coefficient  $r^2$  can be used to evaluate the correlation between the signals.

$$r^2 = \frac{(\sum(x_i - \bar{x})(y_{i+k} - \bar{y}))^2}{(\sum(x_i - \bar{x})^2 \sum(y_{i+k} - \bar{y})^2)} \quad (17)$$

$x$ : average of the first data of signal  $x_i$   
 $y$ : average of the last data of signal  $y_i$   
 $s$ : time shift

Cross-correlation works well if two signals are of the same shape. However, attenuation levels for different frequency components of the shear wave are not the same, and those with high frequencies are more easily attenuated as they travel through the soil media. Thus, the latter parts of the waveform may not match well at all due to different attenuation, as well as due to overlapping signal from nearby refracted and reflected waves. For pseudo-interval CPTu, the

seismic source can also influence the signal shape if it is not very repeatable in generating the shear waves. Therefore, it is impossible for two signals collected at different depths to be of the exactly same shape. Realizing the portions of the signal other than the main wave can affect the value of derived  $V_s$ , Campanella and Stewart (1992) proposed use of a window to select a portion of the signal, which is the main shear wave, while clipping off the latter trailing portions of the signal by setting their amplitudes to zero, (Liao and Mayne).

### 4.3.7 Additional correlations

It is recommended to apply some correlation based on SCPT/CPT results. Four different methods were analyzed and applied to the SCPTu results to compare them to the ones obtained from field test, DeJong. (2007).

For all soils Equation 18, (Mayne, 2006), and Equation 15 (Hegazy and Mayne, 1995), DeJong. (2007):

$$v_s = 118.8 \log_{10}(f_s) + 18.5 \quad (18)$$

$$v_s = [(10.1 \text{Log}_{10} q_t) - 11.4]^{1.67} \left[ 100 \frac{f_s}{q_t} \right]^{0.3} \quad (19)$$

For sand, Equation 20, (Baldi et al., 1989)DeJong. (2007):

$$v_s = 277(q_t)^{0.13}(\sigma'_{vo})^{0.27} \quad (20)$$

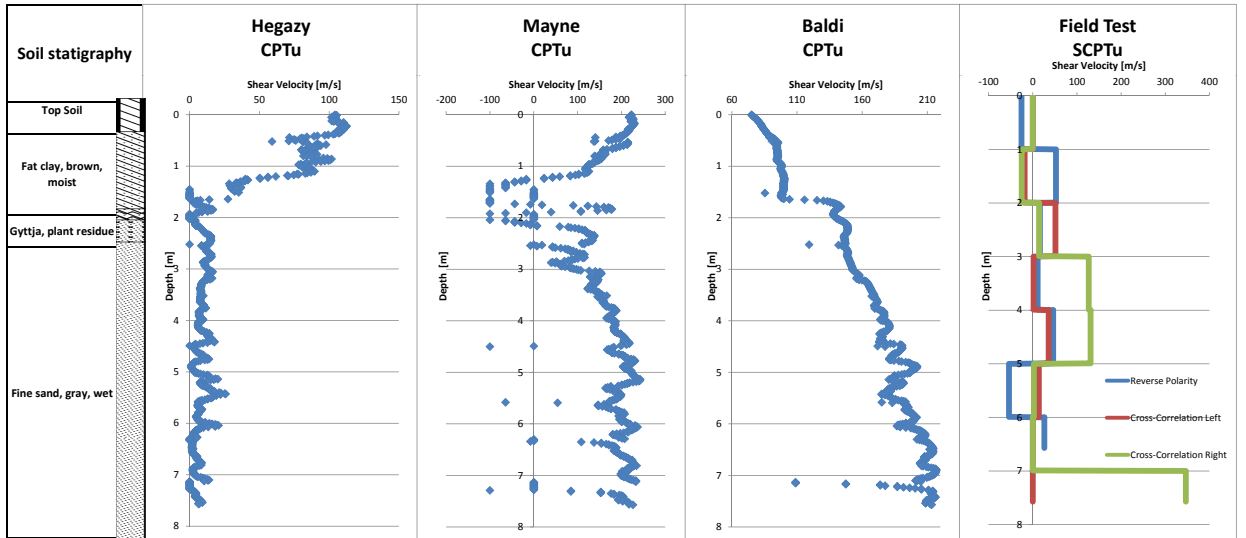
For clay, Equation 21, (Mayne and Rix, 1995), DeJong. (2007):

$$v_s = 1.75(q_t)^{0.627} \quad (21)$$

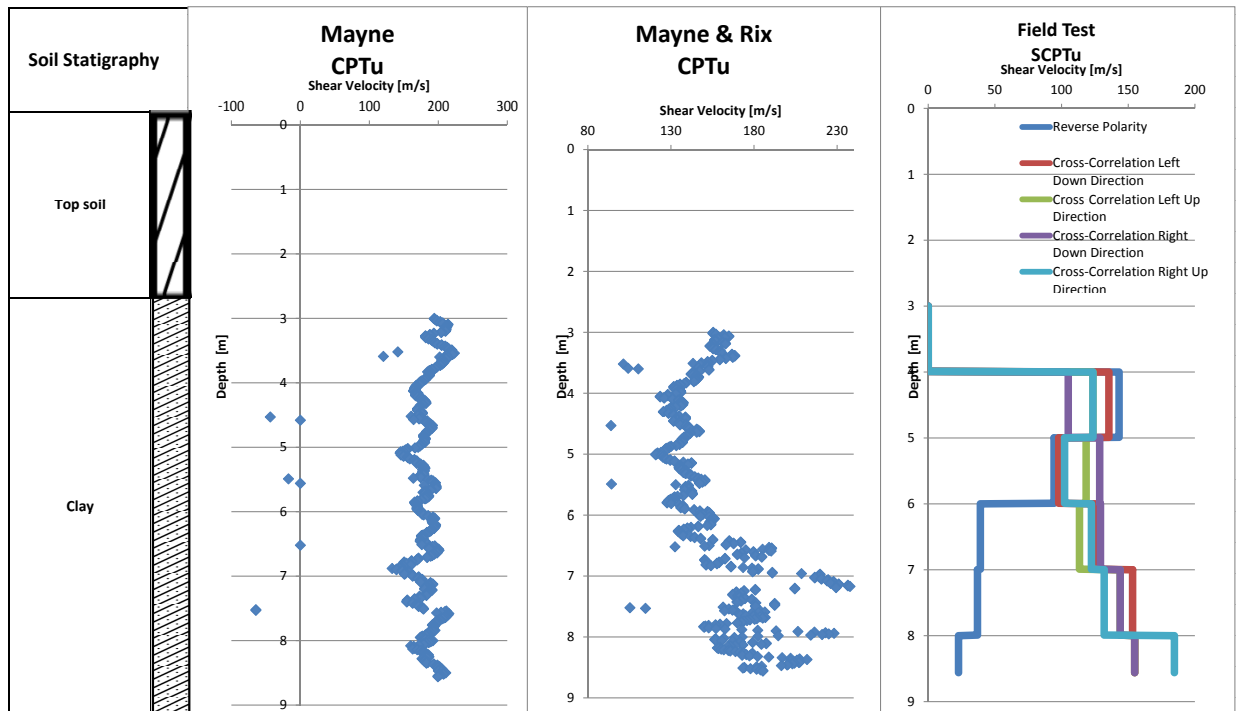
All the results from the empirical methods have been plotted together with the methods used to obtain the SCPTu shear velocities for a better understanding and comparison of the values ranges in Figure 10

The shear velocities formula proposal applied in this article are obtained from DeJong. (2007) and they were created for a certain type of clay and sand. Since this information was used as reference, probably the soils parameters from the soil in Denmark are different from the ones used to create the equations. Thus, it is considered as an inexact method or as an over estimated method.

It can be observed that for sand, SCPTu results from reverse polarity and cross-correlation are in the same of values, except some peaks in the cross-correlation values which can be due to errors in measurements. The reverse polarity, for this sample, has negative shear velocities,



(a) Sand



(b) Clay

Figure 10: Shear velocities obtained from empirical methods and field test results

which are usually in the first meters and the ones obtained in deeper are errors. The right cross-correlation encounter some peak values at 7 meters with can be explained by errors in practical manipulation, since there is a big difference with the left cross-correlation. The reverse polarity gives reasonable values which are in the range given in (Iliescu and Geron). The Mayne and Baldi proposals keep the same range whereas the Hegazy one agrees with the SCPTu field test results.

As for clay, for the SCPTu's more results were compared because as mentioned in (Iliescu and Geron), for one of the SCPTu's it was interesting to consider to perform seismic measurement when the cone was directed both "down" and "up". The cross-correlation results are comparable to the results obtained with the reverse polarization and field test. Unfortunately, for the last meters the results of the reverse polarity and cross-correlation are not matching. The range between the two methods are similar going from 0 to 200 *m/s* which is in the range given by (Iliescu and Geron). As for the empirical results are equivalent but not equivalent to the field test results, although both Mayne's proposals tent to be in the same range of values.

#### 4.3.8 Density

Other value needed to calculate the shear modulus is the density. The density used in this article is given by Equations 23 and 24 which for the over consolidated ratio is needed and it is found by using the Equation 22.

The most common method to estimate OCR and yield stress in fine-grained soils was suggested by Kulhawy and Mayne (1990) (bib) and defined as the ratio of the yield stress and the present effective overburden stress.

$$OCR = \frac{k(q_t - \sigma_{v0})}{\sigma_{v0eff}} \quad (22)$$

*k*: Coefficient [-]

An average value of  $k = 0.33$  can be assumed, with an expected range of 0.2 to 0.5. The higher values of  $k$  are recommended in aged, heavily overconsolidated clays, (DeJong., 2007).

If over consolidated ratio,  $OCR < 2$

$$\rho_r = \frac{\frac{1}{2.41} \log(qc)}{157 \sigma_{v0eff}^{0.65}} \quad (23)$$

And if  $OCR > 2$ , then:

$$\rho_r = \frac{\frac{1}{2.61} \log(qc)}{181 \sigma_m^{0.55}} \quad (24)$$

(T. Lunne, 1997) states that soils with high cone resistance and friction ratio have a high OCR. For both sand and clay, the OCR is  $> 2$ , which was expected and as seen in Section T. Lunne (1997) some of the results are in the overconsolidated areas of the soil classification charts.

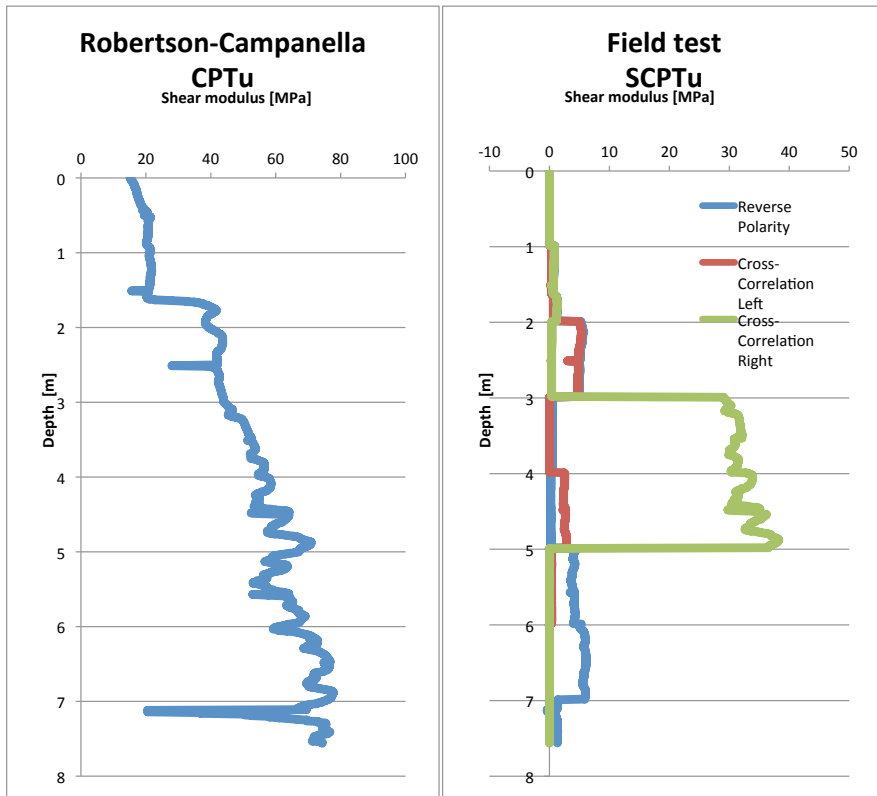
The density obtained from Robertson method, the range is between 0,8 to 2,3 which is a low estimate compared to the values of 2,65 obtained in the lab test for clay as seen in (Iliescu and Geron). Since the lab test was not executed for all the different layers but also for clay, it was not possible to insert the values obtained in the lab which have been more reliable.

#### 4.3.9 Shear Modulus

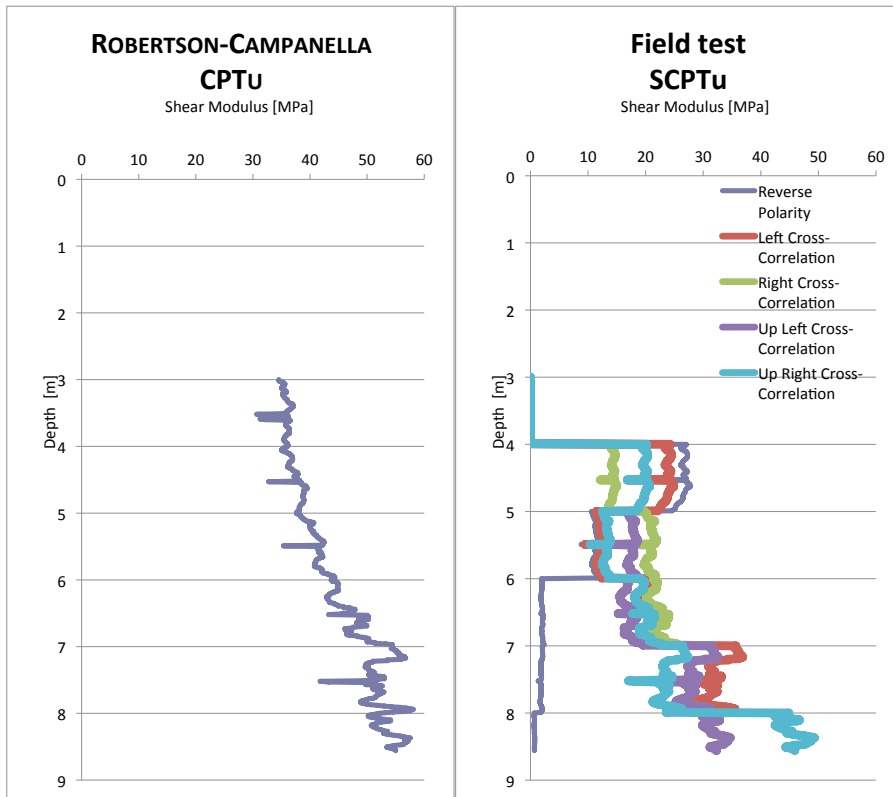
Using Equation (6), shear modulus for fine soils, sand and clay, are obtained from theoretical means, T. Lunne (1997) and SCPTu field data from (Iliescu and Geron), and can be seen in Figure 11

The shear modulus was also computed using a theoretical basis proposed by (P.K.Robertson) and compared with the SCPTu results. The densities obtained from Equation (24) were used for obtaining the results displayed in both charts.

Even thought, for sand it can be observed that the same as in the shear velocities case, cross-correlation left results are not in the same range as the rest of the results, both the empirical method and field test results are in the same range of values. Not the same comment for clay, where the SCPTu results obtained for reverse polarity and cross-correlation (both "down" and "up" direction) are no matching, along with Robertson's empirical proposal values.



(a) Sand



(b) Clay

Figure 11: Shear Modulus results obtained using T. Lunne (1997) and field data, Iliescu and Geron

## 5 Conclusion

A first conclusion to be drawn is that the basic CPTu along with the Seismic test were successful and provided accurate stratigraphic details for both sand and clay. These results were used to carry on the computations and choose the proper formulas in order to obtain the empirical equations. The SCPTu is all in all concluded to be positive and to provide reliable results, regarding the fact that is the first time performed in North of Denmark.

The field test results SCPTu and CPTu estimations are in the same range, as it can be seen in Figure 10. In this paper correction of the measured data according to Robertson has been applied on the CPTu data, thus no error filtering (removing the errors in data due to halts, etc.) of the CPTu data was performed as seen in (Iliescu and Geron). These results are reliable to determine the soil parameters such as the deformation parameters (given by SCPTu) and bearing capacity (given by CPTu) a soil stratigraphy details is also obtained for both sand and clay, for sand lab test results confirm the results obtain for the stratigraphy as seen in Article (Iliescu and Geron).

Concerning the shear velocities, comparing the empirical estimation obtained from the CPTu to the SCPTu field test results, it can be stated that the empirical methods are over estimated. The shear velocities formulas proposals applied are obtained from DeJong. (2007) and they were created based on test for a certain type of soil, that might have not the same properties as the clay and sand found in North of Denmark.

Another important factor that influenced the obtaining of shear modulus, was the density. The values obtained using the (P.K.Robertson) approached were considered to be weak, also taking into consideration that the soil conditions data are different on the site where the tests were performed to the ones that Robertson used.

The final conclusion of this article is the that the shear modulus obtained from both the CPTu (Robertson- Campanella) and the SCPTu results can be considered valid for further research. Even though the density estimations are low, the field test results seem to be the most reliable results since the velocity is more accurate. Overall, the difference between the reverse polarity and cross-correlation is not very significant. It would be good idea for the future researchers to find a possibility to compare further more the methods to observe which one is the most precise one.

## References

- D. Woods R. D. *Screening of the surface wave in soils*. The university of Michigan.
- DeJong., 2007.** Jason T. DeJong. *Site Characterization Guidelines for Estimating Vs Based on In situ Tests*, 2007.
- Dobrin, 1951.** Milton B. Dobrin. *DISPERSION IN SEISMIC SURFACE WAVES*. Geophysics, 16(1), 63–80, 1951. doi: 10.1190/1.1437652. URL <http://link.aip.org/link/?GPY/16/63/1>.
- Iliescu and Geron.** A.I. Iliescu and J. Geron. *Seismic Cone Penetration Test. Experimental results in onshore ares in Northern Denmark*.
- J.A. Jendrecejczuk.** M.W. Wambs  
J.A. Jendrecejczuk. *Surface Measurements of Shear Wave Velocity at The 7-GeV APS Site*. Argonne National Laboratory Report LS-129.
- Liao and Mayne.** T. Liao and P. W. Mayne. *AUTOMATED POST-PROCESSING OF SHEAR WAVE SIGNALS*. Proceedings of the 8th U.S. National Conference on Earthquake Engineering.
- O. and Y.** Magnin O. and Bertrand Y. *Guide Seismique Refraction*. Laboratoire Centrale des ponts et chaussées.
- P.K.Robertson.** P.K.Robertson. *Soil behaviour type from the CPT:an update*. Gregg Drilling and Testing Inc.
- R. G. Campanella, P.K. Robertson.**  
D; Gillespie N. Laing P.J.Kurfurst  
R. G. Campanella, P.K. Robertson. *Seismic cone penetration testing in the near offshore of the MacKenzie Delta*. CAN. GEOTECH. J.
- Rice, 1984.** Anthony H. Rice. *The Seismic Cone Penetrometer*, 1984.
- Seed and Idris.** H. B. Seed and I. M. Idris. *Soil Moduli and Damping Factor for Dynamic Response Analyses*. Report to EERC 70-10, Earthquake Engineering Research Center, Univer. Of California, Berkeley.
- T. Lunne, P.K. Robertson, 1997.**  
J.J.M. Powell T. Lunne, P.K. Robertson. *Cone Penetration Testing in Geotechnical Practice*. ISBN 978-0-419-23750-1, 3. edition. Spon E and F N (UK), 1997.